High stimulus unmasks positive feedback in an autoregulated bacterial signaling circuit

Tim Miyashiro[a] and Mark Goulian[a,b,1]

Departments of [a]Biology and [b]Physics, University of Pennsylvania, Philadelphia, PA 19104

Edited by Thomas J. Silhavy, Princeton University, Princeton, NJ, and approved September 23, 2008 (received for review July 25, 2008)

We examined the effect of positive autoregulation on the steady-state behavior of the PhoQ/PhoP two-component signaling system in *Escherichia coli*. We found that autoregulation has no effect on the steady-state output for a large range of input stimulus, which was modulated by varying the concentration of magnesium in the growth medium. We provide an explanation for this finding with a simple model of the PhoQ/PhoP circuit. The model predicts that even when autoregulation is manifest across a range of stimulus levels, the effects of positive feedback on the steady-state output emerge only in the limit that the system is strongly stimulated. Consistent with this prediction, amplification associated with autoregulation was observed in growth-limiting levels of magnesium, a condition that strongly activates PhoQ/PhoP. In a further test of the model, we found that strains harboring a phosphatase-defective PhoQ showed strong positive feedback and considerable cell-to-cell variability under growth conditions where the wild-type circuit did not show this behavior. Our results demonstrate a simple and general mechanism for regulating the positive feedback associated with autoregulation within a bacterial signaling circuit to boost response range and maintain a relatively uniform and graded output.

autogenous control | PhoP-PhoQ | two-component signal transduction

There is a common perception that positive autoregulation in transcriptional regulatory networks is equivalent to positive feedback and therefore leads to signal amplification or switchlike behavior in the steady-state output. Positive feedback has indeed been observed in autoregulated circuits in numerous systems (e.g., refs. 1–11). However, positive autoregulation does not always bear a simple relation to positive feedback if one of the regulators must be modified (e.g., by phosphorylation) to close the feedback loop and activate transcription. One example of such an autoregulated circuit is the PhoQ/PhoP system, a particularly well-characterized autoregulated two-component signaling system in bacteria (reviewed in refs. 12 and 13). PhoQ, a membrane protein whose activity is modulated by a variety of environmental signals, including Mg^{2+}, pH, and antimicrobial peptides (14–16), autophosphorylates and transfers its phosphoryl group to PhoP (17). In *Escherichia coli*, phosphorylated PhoP (PhoP-P) positively regulates the transcription of multiple genes, including the *phoPphoQ* operon (18, 19). Transcription of *phoPphoQ* is controlled by a constitutive promoter, P2, and a PhoP-dependent promoter, P1 (Fig. 1*A*). Analogous positive autoregulation (i.e., the response regulator activates its own expression and the expression of its cognate histidine kinase) has been reported for numerous other two-component systems and appears to be a common feature of this class of bacterial signaling circuits (e.g., refs. 20–23; reviewed in ref. 11).

Recently, it was shown that autoregulation affects the kinetics of PhoQ/PhoP signaling to produce a surge in response regulator activation (24). Here we focus on the steady-state behavior of autoregulated circuits. Many two-component systems, like PhoQ/PhoP, have a bifunctional histidine kinase, which phosphorylates and dephosphorylates its partner response regulator. In these cases, increased expression of the regulatory proteins affects both the phosphorylation and dephosphorylation reactions, which determine the steady-state level of phosphorylated response regulator. As shown below, this phosphorylation cycle results in a stimulus-dependent effect on positive feedback.

Results and Discussion

To study autoregulation in the context of PhoQ/PhoP signaling, we constructed a set of congenic strains that transcribe the *phoPphoQ* operon from the wild-type autoregulated and constitutive promoters (P1 and P2) or solely from the constitutive promoter (P2) (Fig. 1*B*). We followed PhoP-regulated transcription in single cells using a chromosomal transcriptional fusion of the gene encoding yellow fluorescent protein, *yfp*, to the PhoP-regulated gene *mgrB* (Fig. 1*C*). The strains also contain a chromosomal copy of the gene for cyan fluorescent protein, *cfp*, under the control of a constitutive promoter, which provides an internal normalization for cellular fluorescence (25). Measurements of fluorescence in single cells revealed that PhoP-regulated transcription shows a graded dependence on magnesium over a wide range of concentrations (Fig. 1*C*). When we compared the magnesium-response of autoregulated and non-autoregulated strains, we observed no difference in steady-state transcription for magnesium concentrations down to 30 μM (Fig. 1*C*). This result is not due to the particular transcriptional reporter, because the expression profiles of other PhoP-regulated genes (*hemL*, *mgtA*, and *phoPphoQ*) show a similar insensitivity to autoregulation as well (data not shown).

The equivalent steady-state behavior of the autoregulated and non-autoregulated circuits could simply indicate that, for the above growth conditions, the level of PhoP phosphorylation is insufficient to achieve significant activation of the autoregulated *phoPphoQ* promoter. However, this hypothesis is not consistent with the increase in both PhoP expression and *phoPphoQ* transcription observed at low magnesium (Fig. 1*B* and ref. 19). An alternative explanation is that the increased PhoP expression in the autoregulated circuit does not result in an increased level of phosphorylated PhoP. To explore this possibility in more detail, we modeled the signaling circuit as two interconnected modules, encompassing autoregulation and the phosphorylation cycle (Fig. 2 and supporting information (SI)). For the autoregulation module (Fig. 2*A*), the input is the concentration of PhoP-P ([PhoP-P]) and the outputs are the concentrations of total PhoP ($[PhoP]_{total}$) and total PhoQ ($[PhoQ]_{total}$). We assume the steady-state expression of PhoP and PhoQ have a simple saturating dependence on PhoP-P. The qualitative predictions of the model are insensitive to the particular functional form of this dependence provided it is monotonic and the system operates far from the maximal level of activation of the *phoPphoQ* promoter.

Author contributions: T.M. and M.G. designed research; T.M. performed research; T.M. and M.G. analyzed data; and T.M. and M.G. wrote the paper.

The authors declare no conflict of interest.

This article is a PNAS Direct Submission.

[1]To whom correspondence should be addressed. E-mail: goulian@sas.upenn.edu.

This article contains supporting information online at www.pnas.org/cgi/content/full/0807278105/DCSupplemental.

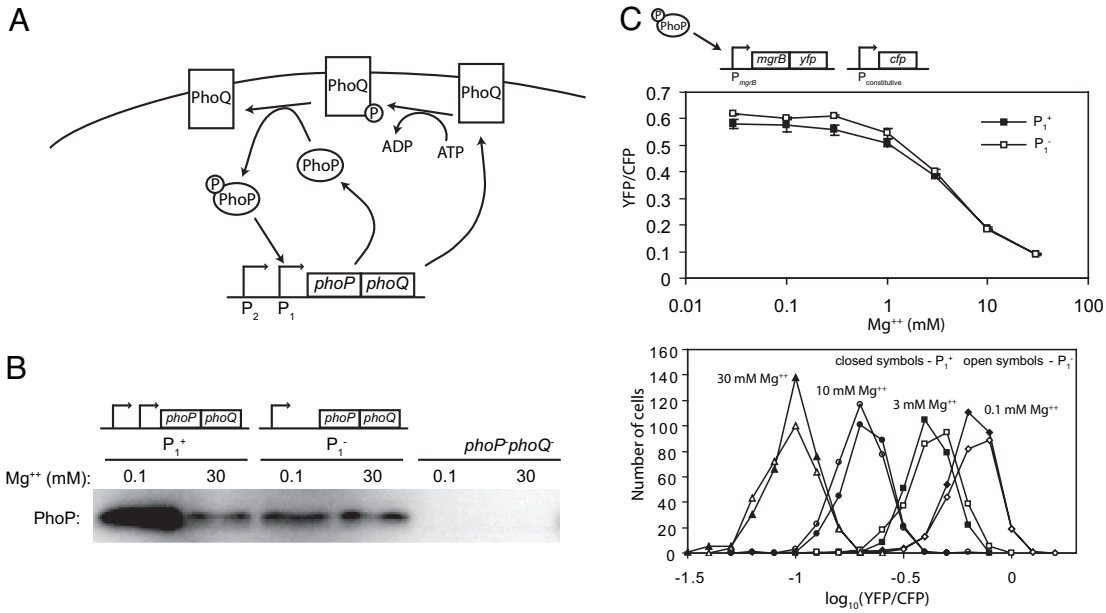

Fig. 1. Positive autoregulation does not affect steady-state PhoQ/PhoP signaling over a wide range of stimuli. (*A*) Positive autoregulation in the PhoQ/PhoP system. The membrane protein PhoQ autophosphorylates and subsequently transfers the phosphoryl group to PhoP. Phosphorylated PhoP activates transcription of *phoPphoQ* from the P1 promoter. The P2 promoter is constitutively active. (*B*) PhoP western blot of autoregulated ($P1^+$), non-autoregulated ($P1^-$), or $phoP^-phoQ^-$ strains (TIM68, TIM69, and TIM13, respectively) grown in the indicated Mg^{2+} concentrations. (*C*) Steady-state PhoP-regulated transcription levels (YFP/CFP) for autoregulated ($P1^+$) or non-autoregulated ($P1^-$) strains (TIM44 and TIM45, respectively) grown in the indicated Mg^{2+} concentrations. Transcription was determined from YFP expressed from a chromosomal operon fusion of *yfp* to the PhoP-regulated gene *mgrB*. The strains also contain a chromosomal copy of *cfp* under control of a constitutive promoter. CFP fluorescence was used as a normalization. (*Above*) Fluorescence ratios were determined from the average of ≈200 cells. Points and bars indicate mean and range for two cultures. (*Below*) Corresponding single-cell distributions for the indicated magnesium concentrations.

Previous work suggests that this is the case for physiologically relevant levels of PhoP-P (19). We also assume that the ratio of protein levels $[PhoP]_{total}/[PhoQ]_{total}$ is constant and much greater than 1. This is consistent with measurements from western blots, from which we have estimated this ratio to be roughly 50 for both 100 μM and growth-limiting levels of magnesium (data not shown). The assumption that the ratio is constant is not important but simplifies the analysis. For the phosphorylation cycle module (Fig. 2*B*), the inputs are PhoQ stimulus (e.g., $[Mg^{2+}]$), $[PhoP]_{total}$, and $[PhoQ]_{total}$. The output, which is [PhoP-P], is set by the cycle of phosphorylation and dephosphorylation by PhoQ. From previous modeling of a two-component system with a bifunctional histidine kinase (26, 27), the levels of [PhoP-P] are expected to saturate with increasing expression of *phoPphoQ* (Fig. 2*B*). This is consistent with the observed saturation of transcription of PhoP-regulated promoters with increasing *phoPphoQ* expression (Fig. 3*B* and 4*C*, blue curve). This saturation has been implicated as a source of robustness to variations in the total levels of response regulator and histidine kinase (26, 27).

The complete PhoQ/PhoP signaling circuit consists of the output and input of the autoregulation module connected to the corresponding input and output of the phosphorylation cycle (Fig. 2*C*). In response to a change in PhoQ stimulus, the circuit adjusts $[PhoP]_{total}$ and $[PhoQ]_{total}$ as well as [PhoP-P]. The steady-state behavior is given by the intersections of the input-output curves for the two modules (Fig. 2*C*). The model assumes that under conditions that weakly stimulate PhoQ, the basal expression of *phoPphoQ* is sufficient to push the level of PhoP-P into saturation. Therefore, further increases in *phoPphoQ* expression from autoregulation have a negligible effect on [PhoP-P] (Fig. 2*C*, compare the [PhoP-P] values of the open and solid squares for the low-stimulus curve). This would account for the observed insensitivity of the output to autoregulation shown in Fig. 1*C*. However, under conditions that strongly stimulate PhoQ, maximal PhoP-P is reached at much higher levels of *phoPphoQ* expression. In this case autoregulation will amplify the level of [PhoP-P]. Thus, our model predicts that positive autoregulation in the PhoQ/PhoP circuit leads to significant positive feedback on the steady-state behavior only in the presence of strong stimulus.

What condition strongly stimulates PhoQ? We found that growth-limiting magnesium levels lead to a marked increase in PhoP-regulated transcription (Fig. 3*A*), which is similar to previous observations for *Salmonella* (28). Importantly, experiments with conditioned media indicate that the PhoQ/PhoP system is in a quasi-steady state under these growth conditions (see SI). This suggests the time scale for reaching steady-state levels of PhoP-regulated transcription is faster than the time scale associated with changes in PhoQ stimulation due to the depletion of magnesium from the media. Under these high-stimulus conditions, PhoP-regulated transcription still shows a saturating dependence on the level of *phoPphoQ* induction (Fig. 3*B*). Furthermore, in contrast with the behavior observed for lower levels of stimulus (Fig. 1*C*), PhoP-regulated transcription is significantly higher in the autoregulated strain compared with the non-autoregulated strain (Fig. 3*A*). Thus, consistent with the prediction of our model, autoregulation has a significant effect on the steady-state output only under conditions of very high stimulus. This elevated level of transcription is apparently important for cell growth in very low (growth-limiting) levels of magnesium because strains that lack *phoPphoQ* autoregulation ($P1^-$) are outcompeted by wild-type strains under these conditions (data not shown).

To further test the model, we explored the effect of perturbing the phosphorylation cycle on the steady-state behavior of the signaling system. According to our model, the saturation of [PhoP-P] with increasing *phoPphoQ* expression (Fig. 2*B Right*) is

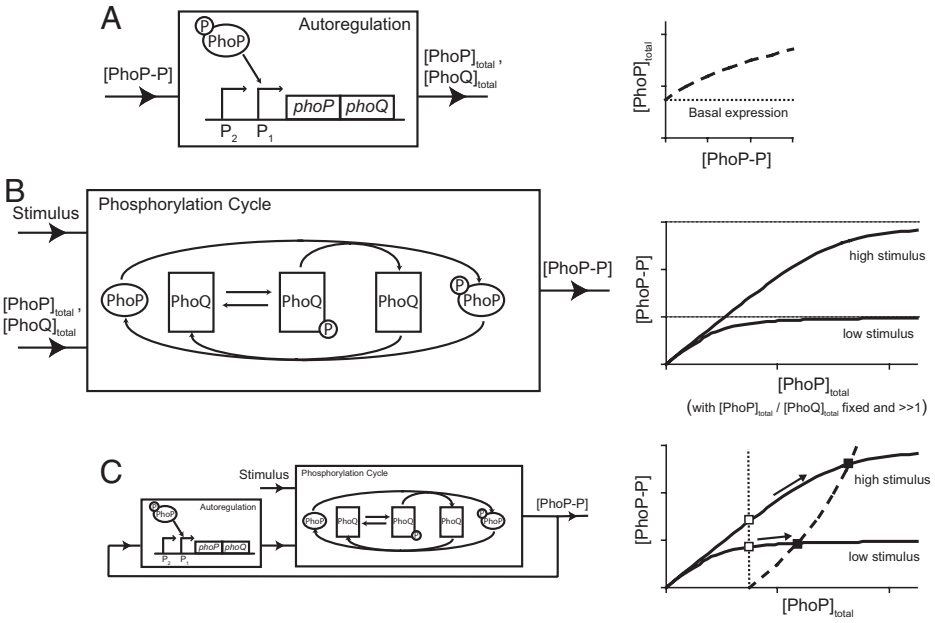

Fig. 2. A model of the PhoQ/PhoP circuit predicts autoregulation will amplify the steady-state output at sufficiently high stimulus. (*A*, *Left*) The autoregulation module determines the total levels of PhoP ($[PhoP]_{total}$) and PhoQ ($[PhoQ]_{total}$) as a function of phosphorylated PhoP ([PhoP-P]). The ratio ($[PhoP]_{total}/[PhoQ]_{total}$) is assumed to be constant and much greater than 1. (*Right*) Steady-state $[PhoP]_{total}$ is taken to be a saturating function of [PhoP-P]. The basal expression level is due to the constitutive promoter P2; the dotted line represents $[PhoP]_{total}$ in a $P1^-$ (non-autoregulated) strain. (*B*, *Left*) The phosphorylation cycle determines [PhoP-P] as a function of stimulus, $[PhoP]_{total}$, and $[PhoQ]_{total}$. The autophosphorylation, phosphotransfer, and phosphatase steps are indicated by the arrows within the box. (*Right*) Steady-state [PhoP-P] saturates as a function of $[PhoP]_{total}$ to a level set by the input stimulus (see SI for details). (*C*, *Left*) the complete circuit consists of the interconnected autoregulation and phosphorylation cycle modules. (*Right*) The steady-state circuit output ([PhoP-P]) is governed by the intersections of the curves in (*A*) and (*B*). Arrows illustrate the amplification in [PhoP-P] due to autoregulation in $P1^+$ strains (closed symbols) vs. $P1^-$ strains (open symbols) for different stimuli. For high-stimulus conditions, the increase in $[PhoP]_{total}$ from autoregulation causes a strong increase in [PhoP-P]. For low-stimulus conditions, the corresponding increase in $[PhoP]_{total}$ does not result in a significant change in [PhoP-P].

due to the cycle of phosphorylation and dephosphorylation of PhoP by PhoQ. A PhoQ variant that lacks phosphatase activity should not show this saturation. Furthermore, the steady-state behavior of the PhoQ/PhoP circuit with such a mutant should be strongly dependent on autoregulation, even for levels of stimulus where autoregulation has no effect on the behavior of the circuit with wild-type PhoQ. To test this, we used a PhoQ(T281R) mutant, which was predicted to have defective phosphatase activity (29). When we compared the activities of cytoplasmic fragments of wild-type PhoQ and PhoQ(T281R) *in vitro*, we found that PhoQ(T281R) showed slower PhoP phosphorylation and no observable PhoP-P dephosphorylation activity (Fig. 4 *A* and *B*).

To test the behavior of full-length PhoQ(T281R) *in vivo*, we compared congenic strains expressing wild-type *phoQ* or *phoQ(T281R)*. Varying the expression of *phoPphoQ(T281R)* from an inducible promoter did not lead to saturation in the transcription of a PhoP-regulated gene (Fig. 4*C*). This result is in marked contrast with the corresponding behavior of wild-type PhoQ and is consistent with the predictions of our model. We also compared the behavior of strains in which *phoPphoQ(T281R)* was expressed from the wild-type (autoregulated) and $P1^-$ (non-autoregulated) promoters for cells growing in 1 mM $[Mg^{2+}]$ (Fig. 4*D Left*). In this case, autoregulation resulted in a roughly 10-fold increase in *mgrB* transcription when compared with the non-autoregulated strain (compare solid and striped red bars in Fig. 4*D Left*). This is again markedly different from the behavior of cells expressing wild-type PhoQ (Fig. 4*D Left*, solid and striped blue bars) and suggests that elimination of PhoQ phosphatase activity results in strong positive feedback, which is consistent with the predictions of our model. Interestingly, the strong positive feedback results in considerable cell-to-cell variability in *mgrB* transcription (Fig. 4*D Right*). The autoregulated $phoQ(T281R)^+$ strain has a remarkably broad histogram of single-cell fluorescence (solid red bars), in contrast with the relatively narrow distributions for the non-autoregulated strain (striped red bars) and for the corresponding strains with wild-type PhoQ (solid and striped blue bars; Fig. 4*D Right*). This behavior of the autoregulated $phoQ(T281R)^+$ strain is also evident on agar plates, where there is considerable variability in YFP fluorescence between colonies (data not shown). Such variability is reminiscent of previous observations of clonal variation associated with the autoregulated PhoR/PhoB two-component system in *E. coli* strains lacking the histidine kinase PhoR (30, 31). Taken together, the above results support the following predictions of our model: (*i*) the cycle of phosphorylation and dephosphorylation leads to a saturated level of PhoP-P with increasing *phoPphoQ* induction, and (*ii*) this PhoQ-controlled saturation limits the positive feedback in the circuit.

Our model captures the basic features of the simplest autoregulated two-component systems containing a bifunctional histidine kinase, which are sufficient for describing the steady-state behavior observed here. We therefore expect that the results will apply to other examples of this class of two-component signaling. More complex systems with additional feedback loops or involving phosphorelays (e.g., refs. 32 and 33) will require additional analysis or alternative models. However, our model is applicable to signaling cascades in which the operon encoding a bifunctional histidine kinase and its partner response regulator is activated by a second regulatory circuit (e.g., refs. 34 and 35). For these cases, the behavior summarized in Fig. 2*B* predicts that increased expression of the two-component signaling proteins will boost the output at high stimulus. This suggests that such cascades of regulatory circuits provide a simple mechanism to modulate the dynamic range of the downstream two-component system through the input stimulus of the up-

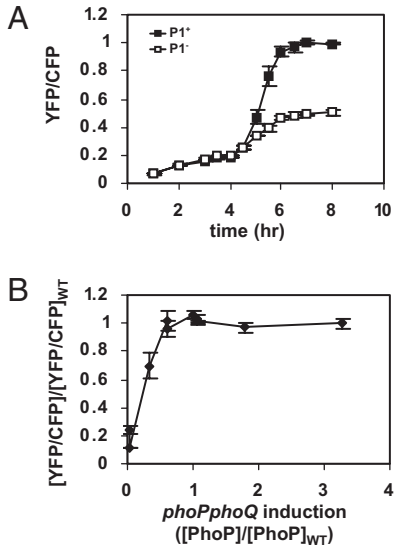

Fig. 3. Autoregulation amplifies PhoP-regulated transcription under conditions of high stimulus associated with growth-limiting [Mg^{2+}]. (*A*) Transcription of the PhoP-regulated *mgrB* promoter (YFP/CFP) for autoregulated ($P1^+$) and non-autoregulated ($P1^-$) strains (TIM44 and TIM45, respectively) cultured in growth-limiting Mg^{2+} concentrations. Fluorescence ratios were determined from the average of ≈200 cells. Points indicate the mean and range for two cultures. (*B*) Transcription of the *mgrB* promoter (YFP/CFP) for cells (TIM219) in growth-limiting Mg^{2+} concentrations with the expression of *phoPphoQ* under IPTG inducible control. The expression of *phoPphoQ* was determined by western blotting against PhoP and normalizing by the level of PhoP in wild-type cells (TIM210) grown under the same condition. Fluorescence ratios were determined from the average of ≈200 cells and normalized by the corresponding ratio for wild-type cells grown under the same condition. Points indicate the mean and range for two cultures.

stream circuit. The model for controlling positive feedback presented here does not depend on the mechanistic details of signal transduction that characterizes two-component systems. Thus, this model can be applied to other biochemical circuits whose saturation behavior shows a similar dependence on the concentrations of regulatory proteins and input stimulus.

Materials and Methods

A brief list of strains is given in Table 1. A detailed description of strain construction is provided in the SI.

Media and Growth Conditions. Cells were grown at 37 °C in minimal A medium (36) (60 mM K_2HPO_4, 33 mM KH_2PO_4, 7.6 mM $(NH_4)_2SO_4$, 1.7 mM sodium citrate) supplemented with 0.1% Casamino acids (BD), 0.2% glucose, and, where not otherwise specified, 1 mM $MgSO_4$. For the experiments shown in Figs. 1 and 4, overnight cultures were diluted 1:1,000 (Figs. 1*B* and 4) or 1:10,000 (Fig. 1*C*) into prewarmed medium and grown for 3.5 h. For the experiments shown in Fig. 3, the overnight cultures were grown in medium containing 1 mM $MgSO_4$ and then diluted 1:1,000 into prewarmed medium containing no added $MgSO_4$ and grown for 8 h.

Fluorescence Measurements. At the indicated time points, samples were rapidly cooled on ice, and streptomycin was added to a final concentration of 250 μg/ml. To immobilize cells against a cover glass, a 5 μl sample was deposited on a slide with a pad of 1% agarose dissolved in minimal medium. For cultures with low optical densities (i.e., $OD_{600} < 0.2$), cells were concentrated before microscopy by spinning at 4 °C and resuspending the pellet in a smaller volume of medium. Fluorescence measurements were obtained using an Olympus IX81 microscope (Olympus America, Inc.) with a 100 W mercury lamp and 100× UPlanApo NA 1.35 objective lens. Filter sets (Chroma) were D436/20 excitation, 455dclp beam splitter, and D480/40 emission for CFP fluorescence measurements; and HQ500/20 excitation, Q5151p beam splitter, and HQ535/30 emission for YFP fluorescence measurements. Images were acquired with a Sensi-

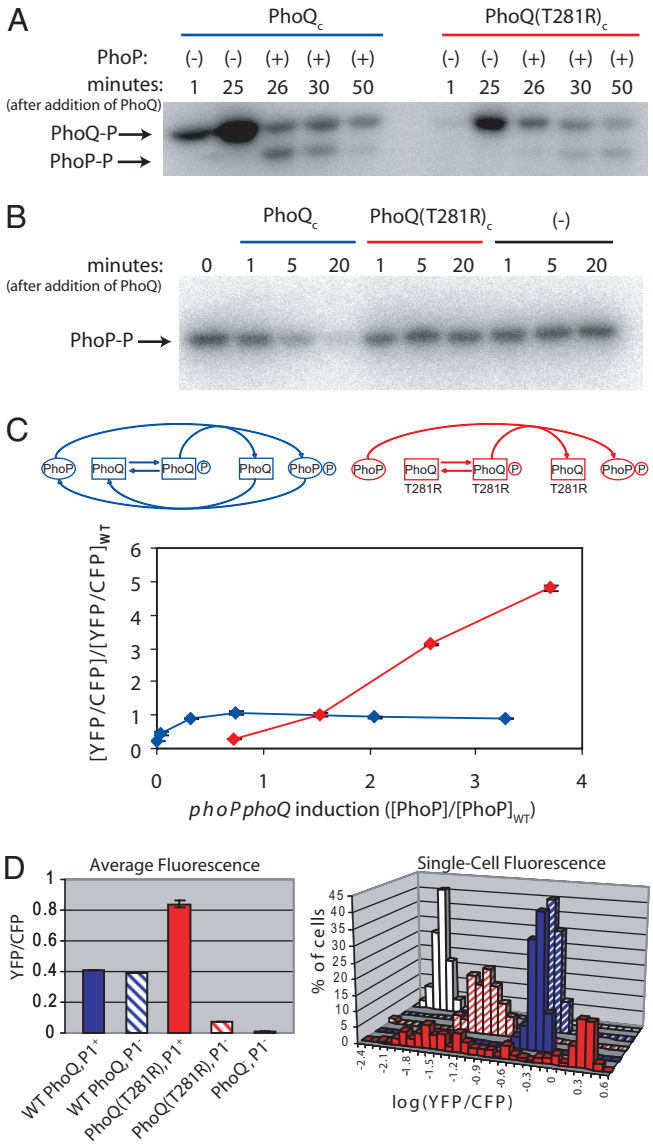

Fig. 4. A phosphatase-defective PhoQ eliminates saturation associated with *phoPphoQ* induction and shows strong positive feedback in an autoregulated strain. (*A*) PhoQ autophosphorylation and phosphotransfer to PhoP for cytoplasmic fragments of wild-type PhoQ and a T281R mutant. PhoP was added after ≈25 min. (*B*) *In vitro* PhoP-P dephosphorylation by cytoplasmic fragments of wild type and a T281R mutant in the presence of ADP. (*C*) Transcription from the *mgrB* promoter (YFP/CFP) for cells grown in 1 mM [Mg^{2+}] with the expression of *phoPphoQ* (blue) or *phoPphoQ(T281R)* (red) under inducible control (strains TIM220 and TIM270, respectively). The induction level of *phoPphoQ* was determined by western blotting against PhoP and normalizing by the level of PhoP in wild-type cells (TIM210) grown under the same condition. Fluorescence ratios were determined from the average of ≈200 cells and normalized by the corresponding ratio for wild-type cells grown under the same condition. Points indicate the mean and range for two cultures. (*D*) Transcription from the *mgrB* promoter (YFP/CFP) for autoregulated ($P1^+$) and non-autoregulated ($P1^-$) strains expressing wild-type *phoPphoQ* or *phoPphoQ(T281R)* grown in 1 mM Mg^{2+}. The strains are TIM284 (solid blue), TIM285 (striped blue), TIM286 (solid red), TIM287 (striped red), and TIM215 (white). (*Left*) Average fluorescence ratios from ≈200 cells (error bars denote the ranges from two cultures). (*Right*) Corresponding histograms of single-cell fluorescence.

Cam QE cooled charge- coupled device camera (Cooke Corporation). Cellular fluorescence was determined using custom software as described in ref. 25.

Protein Purification. To purify PhoP-6xHis, 6xHis-MBP-(EnvZ+MI+loop5), $PhoQ_{cyt}$-6xHis, and $PhoQ(T281R)_{cyt}$-6xHis, 100 ml LB/ampicillin (50 μg/ml) cultures

Table 1. Strains and genotype

Strain	Relevant genotype
MG1655	*rph-1* (*E. coli* Genetic Stock Center, CGSC no. 7740)
TIM13	MG1655 Δ(*P2P1-phoPphoQ*)
TIM44	MG1655 Δ(*P2P1-phoPphoQ*) Φ(*mgrB*$^+$–*yfp*$^+$) *attHK*::[P_{tetA}-*cfp*] *attλ*::[*P2P1-phoPphoQ*]
TIM45	MG1655 Δ(*P2P1-phoPphoQ*) Φ(*mgrB*$^+$–*yfp*$^+$) *attHK*::[P_{tetA}-*cfp*] *attλ*::[*P2-phoPphoQ*]
TIM68	MG1655 Δ(*P2P1-phoPphoQ*) *attλ*::[*P2P1-phoPphoQ*]
TIM69	MG1655 Δ(*P2P1-phoPphoQ*) *attλ*::[*P2-phoPphoQ*]
TIM210	MG1655 Δ*lacZYA attHK*::[P_{tetA}-*cfp*] *attλ*:: [P_{mgrB}-*yfp*]
TIM215	MG1655 Δ(*P2P1-phoPphoQ*) Δ*lacZYA attHK*::[P_{tetA}-*cfp*] *attλ*:: [P_{mgrB}-*yfp*]
TIM219	MG1655 Δ(*P2P1-phoPphoQ*) Δ*lacZYA attHK*::[P_{tetA}-*cfp*] *attλ*:: [P_{mgrB}-*yfp*] *attΦ$_{80}$*::[*lacI^q* P_{trc}-*phoPphoQ*]
TIM220	MG1655 Δ(*P2P1-phoPphoQ*) Δ*lacZYA attHK*::[P_{tetA}-*cfp*] *attλ*:: [P_{mgrB}-*yfp*] *attΦ$_{80}$*::[*lacI^q* P_{trc}*-*phoPphoQ*]
TIM270	MG1655 Δ(*P2P1-phoPphoQ*) Δ*lacZYA attHK*::[P_{tetA}-*cfp*] *attλ*:: [P_{mgrB}-*yfp*] *attΦ$_{80}$*::[*lacI^q* P_{trc}-*phoPphoQ(T281R)*]
TIM284	MG1655 Δ(*P2P1-phoPphoQ*) Δ*lacZYA attHK*::[P_{tetA}-*cfp*] *attλ*:: [P_{mgrB}-*yfp*] *attΦ$_{80}$*::[P_2P_1-*phoPphoQ*]
TIM285	MG1655 Δ(*P2P1-phoPphoQ*) Δ*lacZYA attHK*::[P_{tetA}-*cfp*] *attλ*:: [P_{mgrB}-*yfp*] *attΦ$_{80}$*::[P_2-*phoPphoQ*]
TIM286	MG1655 Δ(*P2P1-phoPphoQ*) Δ*lacZYA attHK*::[P_{tetA}-*cfp*] *attλ*:: [P_{mgrB}-*yfp*] *attΦ$_{80}$*::[P_2P_1-*phoPphoQ(T281R)*]
TIM287	MG1655 Δ(*P2P1-phoPphoQ*) Δ*lacZYA attHK*::[P_{tetA}-*cfp*] *attλ*:: [P_{mgrB}-*yfp*] *attΦ$_{80}$*::[P_2-*phoPphoQ(T281R)*]

of *E. coli* strain BL21(DE3) harboring pTM50, p(6xHis-MBP-EnvZ+MI+loop5), pAN1, and pTM154 were grown at 37 °C to OD_{600} 0.5. IPTG was added to a final concentration of 1 mM, and the cultures were grown for an additional 2–4 h. At that time, cells were harvested, lysed by sonication, and spun at 4 °C for 15 min at 30,000 × *g*. The soluble fraction (≈5 ml) was incubated with 1.25 ml of 50% Ni-NTA agarose (Qiagen) at 4 °C for 1 h. The agarose bed was washed twice and eluted into four 0.5 ml fractions. The purity of the fractions was determined by electrophoresis with 12% SDS-polyacrylamide gels and nonspecific staining of protein with Coomassie. Protein levels were determined by BCA Protein Assay Kit (Pierce). The fractions containing the highest level of each protein were dialyzed into 25 mM Tris-HCl (pH 8.0), 50 mM KCl, 10% glycerol, and stored at 4 °C.

***In Vitro* Phosphorylation Assay.** For the phosphorylation assay shown in Fig. 4*A*, 13 μg PhoQ-6xHis or PhoQ(T281R)-6xHis was autophosphorylated with 100 μM ATP and 10 μCi [γ^{32}P] ATP (3,000 Ci/mmole) in a 20 μl reaction mixture containing reaction buffer (25 mM Tris-Cl [pH 8.0], 50 mM KCl, 1 mM $MgCl_2$, 10% glycerol). The autophosphorylation reaction was initiated by the addition of PhoQ-6xHis or PhoQ(T281R)-6xHis and kept at room temperature. At 1 and 25 min, 2.5 μl of the reaction was removed and added to 2.5 μl reaction buffer and 5 μl 2× SDS-PAGE sample buffer (10% β-mercaptoethanol, 20% glycerol, 4% SDS, 125 mM Tris-HCl [pH 6.8], 0.05% bromophenol blue). At the 25 min time point, 10 μl of each reaction was separately added to tubes containing 5.5 μg PhoP-6xHis in 10 μl reaction buffer and maintained at room temperature. At the times indicated in the figure, 5 μl was removed from each reaction and added to 5 μl 2× SDS-PAGE sample buffer, and 5 μl samples were subjected to electrophoresis on a 12% SDS-PAGE gel. Radioactivity was detected using a phosphor screen and Storm imager (GE Healthcare).

***In Vitro* Phosphatase Assay.** For the phosphatase assay shown in Fig. 4*B*, we used an EnvZ chimera, EnvZ+MI+loop5 (37) to phosphorylate PhoP. This protein efficiently phosphorylates PhoP *in vitro* and does not show significant PhoP-P phosphatase activity. It is therefore a convenient means for producing high levels of PhoP-P *in vitro*. Thirty-three micrograms of 6xHis-MBP-(EnvZ+MI+loop5) was first autophosphorylated with 100 μM ATP and 25 μCi [γ^{32}P] ATP (3000 Ci/mmole) in a 40 μl reaction mixture containing reaction buffer (same buffer as described previously). The autophosphorylation reaction was initiated by the addition of 6xHis-MBP-(EnvZ+MI+loop5) and kept at room temperature for 20 min. After 20 min, 30 μl of the reaction was transferred to a tube containing 56 μg PhoP-6xHis in 30 μl reaction buffer and kept at room temperature for 40 min to phosphorylate PhoP-6xHis. After 40 min, 50 μl of the reaction was applied to an Illustra ProbeQuant G-50 Micro Column (GE Healthcare) to remove unincorporated ATP. Approximately 15 μl of the flow-through (containing phosphorylated PhoP-6xHis) was added to tubes with 15 μl reaction buffer containing 4.7 μg $PhoQ_{cyt}$-6xHis + 200 μM ADP, 14.7 μg $PhoQ_{cyt}$(T281R)-6xHis + 200 μM ADP, or 200 μM ADP. At each time point, 5 μl samples were transferred to tubes containing 5 μl 2× SDS-PAGE sample buffer, and 7.5 μl samples were subjected to electrophoresis on a 12% SDS-PAGE gel. Radioactivity was detected using a phosphor screen and Storm imager.

ACKNOWLEDGMENTS. We thank J. Zhu for help with phosphorylation assays, M. Laub for the EnvZ+MI+Loop5 chimera, and A. Binns, A. Vollmer, C. Waldburger, M. van der Woude, and members of the Goulian and Binns labs for helpful discussions. This work was supported by National Science Foundation Grant MCB0212925 and National Institutes of Health Grant GM080279 (to M.G.) and an American Heart Association predoctoral fellowship (to T.M.).

1. Becskei A, Seraphin B, Serrano L (2001) Positive feedback in eukaryotic gene networks: Cell differentiation by graded to binary response conversion. *EMBO J* 20:2528–2535.
2. Ferrell JE, Jr (2002) Self-perpetuating states in signal transduction: Positive feedback, double-negative feedback and bistability. *Curr Opin Cell Biol* 14:140–148.
3. Hasty J, Pradines J, Dolnik M, Collins JJ (2000) Noise-based switches and amplifiers for gene expression. *Proc Natl Acad Sci USA* 97:2075–2080.
4. Isaacs FJ, Hasty J, Cantor CR, Collins JJ (2003) Prediction and measurement of an autoregulatory genetic module. *Proc Natl Acad Sci USA* 100:7714–7719.
5. Ozbudak EM, Thattai M, Lim HN, Shraiman BI, Van Oudenaarden A (2004) Multistability in the lactose utilization network of Escherichia coli. *Nature* 427:737–740.
6. Maamar H, Dubnau D (2005) Bistability in the Bacillus subtilis K-state (competence) system requires a positive feedback loop. *Mol Microbiol* 56:615–624.
7. Smits WK, *et al.* (2005) Stripping Bacillus: ComK auto-stimulation is responsible for the bistable response in competence development. *Mol Microbiol* 56:604–614.
8. Veening JW, Hamoen LW, Kuipers OP (2005) Phosphatases modulate the bistable sporulation gene expression pattern in Bacillus subtilis. *Mol Microbiol* 56:1481–1494.
9. Suel GM, Garcia-Ojalvo J, Liberman LM, Elowitz MB (2006) An excitable gene regulatory circuit induces transient cellular differentiation. *Nature* 440:545–550.
10. Alon U (2007) Network motifs: Theory and experimental approaches. *Nat Rev Genet* 8:450–461.
11. Mitrophanov AY, Groisman EA (2008) Positive feedback in cellular control systems. *Bioessays* 30:542–555.
12. Groisman EA (2001) The pleiotropic two-component regulatory system PhoP-PhoQ. *J Bacteriol* 183:1835–1842.
13. Ernst RK, Guina T, Miller SI (2001) Salmonella typhimurium outer membrane remodeling: Role in resistance to host innate immunity. *Microbes Infect* 3:1327–1334.
14. Garcia Vescovi E, Soncini FC, Groisman EA (1996) Mg2+ as an extracellular signal: Environmental regulation of Salmonella virulence. *Cell* 84:165–174.
15. Prost LR, *et al.* (2007) Activation of the bacterial sensor kinase PhoQ by acidic pH. *Mol Cell* 26:165–174.
16. Bader MW, *et al.* (2005) Recognition of antimicrobial peptides by a bacterial sensor kinase. *Cell* 122:461–472.
17. Castelli ME, Garcia Vescovi E, Soncini FC (2000) The phosphatase activity is the target for Mg2+ regulation of the sensor protein PhoQ in Salmonella. *J Biol Chem* 275:22948–22954.
18. Kato A, Tanabe H, Utsumi R (1999) Molecular characterization of the PhoP-PhoQ two-component system in Escherichia coli K-12: Identification of extracellular Mg2+-responsive promoters. *J Bacteriol* 181:5516–5520.
19. Miyashiro T, Goulian M (2007) Stimulus-dependent differential regulation in the Escherichia coli PhoQ PhoP system. *Proc Natl Acad Sci USA* 104:16305–16310.
20. Scarlato V, Prugnola A, Arico B, Rappuoli R (1990) Positive transcriptional feedback at the bvg locus controls expression of virulence factors in Bordetella pertussis. *Proc Natl Acad Sci USA* 87:6753–6757.
21. Reitzer LJ, Magasanik B (1983) Isolation of the nitrogen assimilation regulator NR(I), the product of the glnG gene of Escherichia coli. *Proc Natl Acad Sci USA* 80:5554–5558.
22. Guan CD, Wanner B, Inouye H (1983) Analysis of regulation of phoB expression using a phoB-cat fusion. *J Bacteriol* 156:710–717.
23. Hoch JA, Silhavy TJ (1995) *Two-Component Signal Transduction* (ASM Press, Washington, DC).
24. Shin D, Lee EJ, Huang H, Groisman EA (2006) A positive feedback loop promotes transcription surge that jump-starts Salmonella virulence circuit. *Science* 314:1607–1609.
25. Miyashiro T, Goulian M (2007) Single-cell analysis of gene expression by fluorescence microscopy. *Methods Enzymol* 423:458–475.

26. Batchelor E, Goulian M (2003) Robustness and the cycle of phosphorylation and dephosphorylation in a two-component regulatory system. *Proc Natl Acad Sci USA* 100:691–696.
27. Shinar G, Milo R, Martinez MR, Alon U (2007) Input output robustness in simple bacterial signaling systems. *Proc Natl Acad Sci USA* 104:19931–19935.
28. Tao T, Grulich PF, Kucharski LM, Smith RL, Maguire ME (1998) Magnesium transport in Salmonella typhimurium: Biphasic magnesium and time dependence of the transcription of the mgtA and mgtCB loci. *Microbiology* 144(Pt 3):655–664.
29. Shin D, Groisman EA (2005) Signal-dependent binding of the response regulators PhoP and PmrA to their target promoters in vivo. *J Biol Chem* 280:4089–4094.
30. Wanner BL (1987) Control of phoR-dependent bacterial alkaline phosphatase clonal variation by the phoM region. *J Bacteriol* 169:900–903.
31. Zhou L, Grégori G, Blackman JM, Robinson JP, Wanner BL (January 28, 2005) Stochastic activation of the response regulator PhoB by noncognate histidine kinases. *Journal of Integrative Bioinformatics* 2:11.
32. Raivio TL, Popkin DL, Silhavy TJ (1999) The Cpx envelope stress response is controlled by amplification and feedback inhibition. *J Bacteriol* 181:5263–5272.
33. Williams CL, Cotter PA (2007) Autoregulation is essential for precise temporal and steady-state regulation by the Bordetella BvgAS phosphorelay. *J Bacteriol* 189:1974–1982.
34. Oshima T, *et al*. (2002) Transcriptome analysis of all two-component regulatory system mutants of Escherichia coli K-12. *Mol Microbiol* 46:281–291.
35. Bijlsma JJ, Groisman EA (2003) Making informed decisions: Regulatory interactions between two-component systems. *Trends Microbiol* 11:359–366.
36. Miller JH (1992) *A Short Course in Bacterial Genetics: A Laboratory Manual and Handbook for Escherichia Coli and Related Bacteria* (Cold Spring Harbor Laboratory Press, Plainview, NY).
37. Skerker JM, *et al*. (2008) Rewiring the specificity of two-component signal transduction systems. *Cell* 133:1043–1054.